AD_____

Award Number: DAMD17-00-1-0343

TITLE: Organic Polymer Light Emitting Display for Digital Mammography

PRINCIPAL INVESTIGATOR: Dr. Joohan Kimis

CONTRACTING ORGANIZATION: The University of Michigan
Ann Arbor, Michigan 48109-1274

REPORT DATE: March 2002

TYPE OF REPORT: Annual Summary

PREPARED FOR: U.S. Army Medical Research and Materiel Command
Fort Detrick, Maryland 21702-5012

DISTRIBUTION STATEMENT: Approved for Public Release;
Distribution Unlimited

The views, opinions and/or findings contained in this report are those of the author(s) and should not be construed as an official Department of the Army position, policy or decision unless so designated by other documentation.

REPORT DOCUMENTATION PAGE

1. AGENCY USE ONLY (Leave blank)	2. REPORT DATE March 2002	3. REPORT TYPE AND DATES COVERED Annual Summary (1 Mar 01 – 28 Feb 02)	

4. TITLE AND SUBTITLE
Organic Polymer Light Emitting Display for Digital Mammography

5. FUNDING NUMBERS
DAMD17-00-1-0343

6. AUTHOR(S)
Dr. Joohan Kimis

7. PERFORMING ORGANIZATION NAME(S) AND ADDRESS(ES)
The University of Michigan
Ann Arbor, Michigan 48109-1274

E-Mail: agb@cdrh.fda.gov

8. PERFORMING ORGANIZATION REPORT NUMBER

9. SPONSORING / MONITORING AGENCY NAME(S) AND ADDRESS(ES)
U.S. Army Medical Research and Materiel Command
Fort Detrick, Maryland 21702-5012

10. SPONSORING / MONITORING AGENCY REPORT NUMBER

11. SUPPLEMENTARY NOTES

12a. DISTRIBUTION / AVAILABILITY STATEMENT
Approved for Public Release; Distribution Unlimited

12b. DISTRIBUTION CODE

13. ABSTRACT (Maximum 200 Words)

We have developed simulation tools for the optimization of the organic light-emitting device (OLED) high-resolution monochrome structures for medical imaging applications. We studied the effect of thin-film coatings and optical absorption in the organic materials on the emitted OLED spectra.
We investigated advanced measurement methods for the characterization of display prototypes that will be fabricated in the University of Michigan laboratories.
Using measured optical properties of the materials involved in a typical OLED structure, we computed the color shift from the photo-luminescent spectrum. In a submitted manuscript, we reported on the Monte Carlo method for modeling light transport phenomena in multi-layer organic polymer light-emitting devices on plastic substrates.
We find that for all polymers considered, the emission is shifted toward the longer wavelengths, and that the shift is maximum for emissions with peaks around 530 nm.
The photon extraction efficiency is higher (0.430) for polymers emitting in the longer wavelengths, while the absorbed fraction is higher (0.676) for spectra with maximum in the short wavelengths.

14. SUBJECT TERMS
electronic display, light-emitting polymers, mammography

15. NUMBER OF PAGES
20

16. PRICE CODE

17. SECURITY CLASSIFICATION OF REPORT Unclassified	18. SECURITY CLASSIFICATION OF THIS PAGE Unclassified	19. SECURITY CLASSIFICATION OF ABSTRACT Unclassified	20. LIMITATION OF ABSTRACT Unlimited

Contents

3 Introduction

Commercially available display devices for use in digital mammography systems are known to have less image quality than the mammographic transilluminated film. Performance parameters that have been recognized as poor include low maximum luminance, reduced luminance range, veiling glare and ambient light reflections, insufficient resolution, and phosphor granularity noise, among others. However, it will bep ossible to achieve, with an electronic display, better image quality than that observed with radiographic film. Organic polymer light-emitting displays (OLEDs) are all-solid-state flat panel devices that emit light through electron-hole recombination processes. Recently, OLEDs have received worldwide attention, because of their high luminous efficiency that can be achieved at room temperature with low driving voltages. A display device that delivers better image quality than the "gold standard" for mammography digital systems would allow a much more rapid and decisive deployment of fully digital solutions for the detection of breast cancer. The use of a display that could achieve a maximum luminance higher than 2,000 cd/m^2 while having a very low minimum luminance would allow the radiologists to implement image processing techniques that benefit from the extended luminance range. Such a display would allow for film-less practice without sacrificing diagnostic performance.

4 Body

The electronic display of mammographic images remains today an important technological barrier for the deployment of fully digital mammography systems. Extremely good spatial resolution in large image pixel array sizes are required to detect and characterize small lesions. In addition, good contrast resolution is needed to achieve high diagnostic performance when subtle details are present in low-luminance image regions [1, 2]. During this project, we have achieved the following objectives:

1. **Improve available simulation methods for OLED modeling** by incorporating actual photon luminescent spectra characteristics and optical material properties of OLED materials used in the University of Michigan laboratory.

2. **Optimization of OLED optical performance:** We have used advanced computational modeling tools to predict the achievable improvements and define new structures by studying the effect of surface and material properties on the optical performance of AM-OLEDs.

3. **Simulation of the OLED bidirectional reflection distribution function:** We have modeled the reflection signatures of OLEDs.

4. **Simulation of the OLED luminance emission angular distribution.:** We measured and modeled the angular luminance emission distributions of typical OLED structures.

4.1 Simulation methods

After the simple analysis of OLED efficiency presented in Ref. [3], several groups have investigated the effect of light transport in multi-layer structures [4–7]. The method we developed, is based on

4

a Monte Carlo (MC) approach [8,9]. The MC method makes use of the generation of photons with random direction according to a distribution function describing the nature of the light emission. In this analysis, the light source within the organic polymer layer is considered isotropic from a single point situated in the center of the device. The method is described in detail in Ref. [10] (see Appendix).

4.2 Optimization of the device efficiency

We measured the index of refraction, absorption, photoluminescence (PL), and electro-luminescence (EL) of three organic polymers (A, B, and C) with peak emission in a different region of the visible spectrum. The OLED structure modeled is a hetero-structure OLED described by [11] with an aluminum cathode electrode and a transparent anode ITO electrode (160 nm, refractive index 1.8). The organic polymer film thickness used was 200 nm. The transparent substrate index of refraction was 1.5 and its thickness 900 μm.
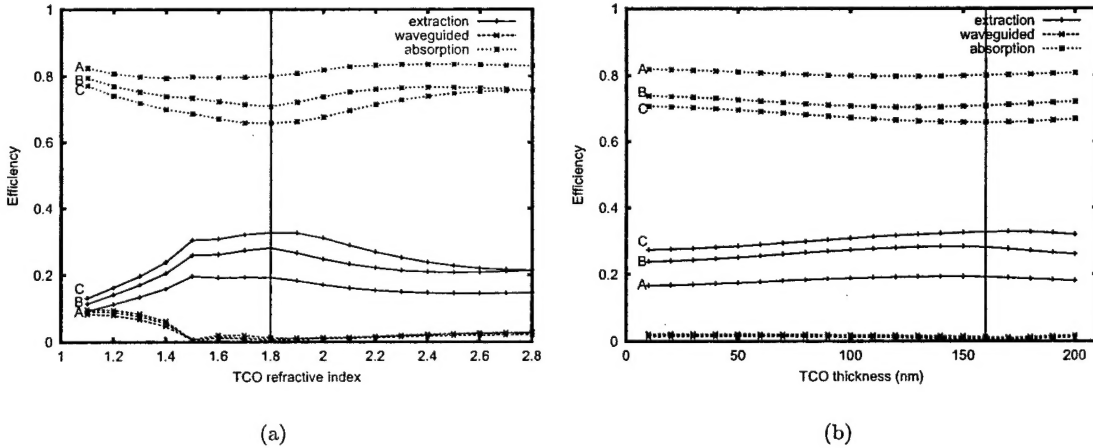

(a)   (b)

Figure 1: Extraction efficiency η_{pe}, waveguiding η_{wa} and absorption η_{ab} for different transparent conductive oxide (TCO) electrode models (see Ref. [12] for details).

In Fig. 1, we present results showing the change in the values of η_{pe}, η_{ab}, and η_{wa} with the index of refraction (thickness) of the transparentcond ucting oxide (TCO) electrode covering the range from 1.1 to 2.7 (10-200 nm). We find that both the thickness and refractive index of the transparent electrode have a minor effect on the shift of the SL spectrum with respect to the PL emission. We obtained a maximum η_{pe} for TCO thickness and refractive index of about 170 nm and 1.85 respectively. The waveguide modes are determined by the geometry of the OLED stack that defines a total internal reflection angle (α_{TIR}) with respect to the device plane, beyond which all photons are emitted through the edges. Since our source of photons is isotropic, we expect lower η_{wa} for larger devices due to: (1) increased probability of reflection and scattering going into the solid angle defined by α_{TIR}, and (2) increased absorption in the organic polymer layer. For all organic polymers considered in this work, our results show that the simulated light emission is shifted toward the longer wavelengths consistently with experimental measurements of EL. We

also show that the photon extraction efficiency is reduced by light absorption and waveguiding. The reduction of the OLED wave-guided fraction can be obtained by using structured substrates, or by tuning the refractive index of the layers to maximize transmission and reduce total internal reflection at each interface.

4.3 Reflection properties of OLEDs

The effective physical contrast of display devices is affected by the achievable contrast generated by the light-producing or light-modulating elements, and by reflections of ambient light. In emissive displays that are typically highly reflective by design, the control of ambient light reflection is critical to achieve high contrast, especially when large luminance dynamic range is needed. For instance, in high-performance medical imaging cathode-ray tubes (CRTs), the glass faceplate is darkened to reduce diffuse reflections and is coated with an anti-reflection film to reduce the specular component. In this phase of the project, paper, we developed a computational method for modeling the BRDF of electronic displays that relies on an optical Monte Carlo simulation code developed to study light transport processes in emissive structures. The BRDF calculations are based on a Monte Carlo (MC) method developed for studying light transport effects in emissive structures [8]. The BRDF, a formalism often used in optics [13], is defined by a six-dimensional function:

$$BRDF(\theta_i, \phi_i, \theta_o, \phi_o, \lambda, p) = \frac{dL_o(\theta_o, \phi_o, \lambda, p)}{dE_i(\theta_i, \phi_i, \lambda, p)} \qquad (1)$$

where λ is the photon wavelength and p is the polarization of the incoming light beam. The BRDF has units of sr^{-1}. The angle of incidence of ambient light is defined by (θ_i, ϕ_i), while (θ_o, ϕ_o) are the angles that define the direction of reflected light.

The precise evaluation of this function is time consuming and costly. The BRDF can be measured with a goniometric setup with fixed light source and variable detector, with variable source and fixed detector, or with a conoscopic approach where the directional intensity is mapped into a two-dimensional distribution recorded by a position-sensitive planar detector. The first two methods suffer from severe dependence of source and detector positioning precision which has to be less than 1°. The third method requires expensive instrumentation. The models of display devices are based on uniform slabs representing multiple material layers.

In this study, we consider only the integrated response to an unpolarized light source with flat spectrum in the range from 400 to 800 nm. Finally, the angular distribution function contained in equally spaced bins from the Monte Carlo simulations is reduced to a luminance distribution density in the range of $[0, 90°]$ for a given incidence angle α_i with a factor $1/cos(\alpha_o)$. The introduction of this factor is needed to directly relate the distribution density in angles with the expected angular variations in the luminance out of the device (L). $B^{\alpha_i}(\alpha_o)$ is also known as the in-plane or two-dimensional BRDF. Eq. 2 shows the final metric computed from the Monte Carlo simulations.

$$B^{\alpha_i}(\alpha_o) = \frac{dL(\alpha_o)/cos(\alpha_o)}{dE(\alpha_i)} \qquad (2)$$

Organic light-emitting displays are simulated using a typical structure model that includes measured optical properties for the organic polymer films and the substrate [10]. The OLED model
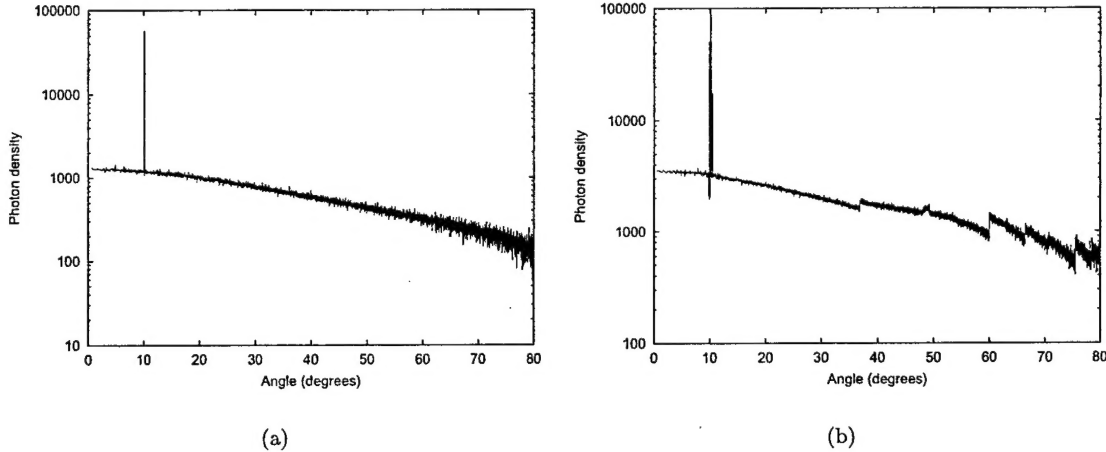
6

Figure 2: $B^{10}(\alpha_o)$ for (a) a monochrome CRT with geometrical and material models described in [8], and (b) for an OLED device with geometrical and material models described in [10].

represents a hetero-structure OLED described by He *et al.* [11] with an aluminum cathode electrode and a transparent anode ITO electrode (160 nm, refractive index 1.8). The organic polymer film thickness used was 200 nm. The substrate index of refraction was 1.5 and its thickness 900 μm. Fig. 2 shows $B^{10}(\alpha_o)$ for OLEDs. It can be observed that the specular component is predominant ($R_S = 0.10$, $R_D = 0.06 \ sr^{-1}$). The results reveal that the specular peak has a significant width.

We performed preliminary experimental measurements of the OLED's BRDF using a highly accurate BRDF setup at the National Institute of Standards and Technology (NIST) in the Flat Panel Display Measurements Laboratory (directed by Ed Kelley). In Fig. 3 we show a comparison of the experimental high resolution BRDF data with the predictions of the simulation. In summary, we have showed that the BRDF of OLED displays based on polymer films backed with a metallic reflective electrode is highly specular. We reported for the first time the complete BRDF signature of OLEDs, showing that the haze component is small, with a characteristic width of 2°. This intermediate component

Figure 3: Comparison of high resolution BRDF measurements with simulated results for typical OLEDs.

of reflection complicates the measurement of the specular peak since luminance meters having slightly different apertures will produce a specular reflection component with large errors. The experimental results agree with the simulation predictions well within the experimental uncertainties present in even high resolution BRDF measurement setups.
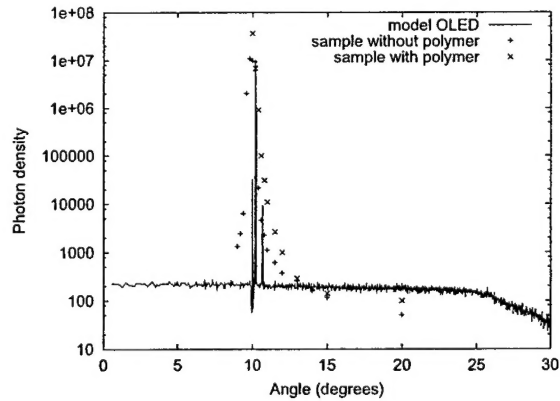
4.4 Angular luminance emission of OLEDs

We investigated the light emission angular distribution of the OLEDs. We found that the angular distribution of the luminance is pseudo-Lambertian (rather than Lambertian) with increased intensity in the forward direction, Fig. 4. It was found that the light refraction at different interfaces, and the mirror-like nature of the bottom surface lead to this forward-peaked angular distribution, while the absorption represent a minor effect. Finally, it is clear from our simulation that the waveguiding effect cannot be neglected in the OLEDs and its contribution will be dependenton substrate thickness and refractive index values (see Appendix).
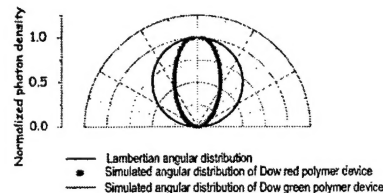

Figure 4: Simulated angular luminance distributions of OLEDs for different emissive polymers.

5 Key Research Accomplishments

In this project, we have achieved the following accomplishments:

1. **Development of improved simulation methods for OLED modeling** by incorporating actual photon luminescent spectra characteristic of OLED materials used in the University of Michigan laboratory.

2. **Simulation and optimization of OLED optical performance** with respect to color shift of photoluminescent spectra, reflection properties, and angular luminance distribution.

6 Reportable Outcomes

During the project, the simulation code was improved and ported to Windows-based computers and a variety of Unix machines (Sun UltraSparc 10, HP Vectra, etc). We generated one manuscript that was published in the Journal of Applied Physics [10], and two presentations [?, 14] (see Appendix). Another manuscript is in preparation [15]. The simulation code DETECT-II is available to other investigators on a "as-is" basis. For information, contact Dr. Aldo Badano (agb@cdrh.fda.gov).

References

[1] K. Doi, M. L. Giger, R. M. Nishikawa, and R. A. Schmidt, eds., *Digital mammography*, ch. Technical aspects of digital mammography, pp. 33–41. Elsevier Science, 1996.

[2] L. L. Fajardo and M. B. Williams, *Digital mammography*, ch. The clinical potential of digital mammography, pp. 43–52. Elsevier Science, 1996.

[3] N. C. Greenham, S. C. Moratti, D. D. C. Bradley, *et al. Nature* **365**, p. 628, 1993.

[4] G. Gu, D. Z. Garbuzov, P. E. Burrows, S. Venkatesh, and S. R. Forrest, "High-external-quantum-efficiency organic light-emitting devices," *Optics Letters* **22**(6), pp. 396–398, 1997.

[5] S. E. Burns, G. Denton, N. Tessler, F. Cacialli, *et al.*, "High finesse organic microcavities," *Optical Materials* **9**, pp. 18–24, 1998.

[6] V. Bulović, V. B. Khalfin, G. Gu, P. E. Burrows, D. Z. Garbuzov, and S. R. Forrest, "Weak microcavity effects in organic light-emitting diodes," *Physical Review B* **58**(7), 1998.

[7] F. Cacialli, S. E. Burns, and H. Becker, "Interference phenomena in polymer light-emitting diodes: photoluminescence and modelling," *Optical Materials* **9**, pp. 168–172, 1998.

[8] A. Badano, *Image Quality Degradation by Light Scattering Processes in High Performance Display Devices for Medical Imaging.* PhD thesis, University of Michigan, 1999.

[9] G. F. Knoll and T. F. Knoll, "Light collection in scintillation detector composites for neutron detection," *IEEE Transactions on Nuclear Science* **35**, pp. 872–875, July 1988.

[10] A. Badano and J. Kanicki, "Monte Carlo analysis of the spectral photon emission and extraction efficiency of organic light-emitting devices," *Journal of Applied Physics* **90**(4), 2001.

[11] Y. He, S. Gong, R. Hattori, and J. Kanicki *Applied Physics Letters* **74**, 1999.

[12] A. Badano and J. Kanicki, "Characterization of crosstalk in high-resolution active-matrix liquid crystal displays for medical imaging," *Proc. of the SPIE* **4295**, 2001.

[13] M. Elias, L. Simonot, and M. Menu, "Bidirectional reflectance of a diffuse background covered by a partly absorbing layer," *Optics Communications* **191**, pp. 1–7, 2001.

[14] S.-J. Lee, A. Badano, Y. Hong, and J. Kanicki, "Monte Carlo simulation of spectral photon emission of the organic polymer light emitting devices," in *International Conference of Electroluminescence*, 2001.

[15] A. Badano, "Modeling the bidirectional relflectance of display devices," *To be published in Applied Optics* , 2001.

7 Appendices

Abstract and Poster presented at ICEL'01, Los Angeles, CA, 2001.

Proceedings paper presented at the International Display Research Conference, Osaka, Japan, 2001.

Reprint from Journal of Applied Physics: "MONTE CARLO ANALYSIS OF THE SPECTRAL PHOTON EMISSION AND EXTRACTION EFFICIENCY OF ORGANIC LIGHT-EMITTING DEVICES".

Bidirectional Reflectance of Organic Light-Emitting Displays

Aldo Badano, Shu-Jen Lee, Jerzy Kanicki, Edward F. Kelley and Robert J. Jennings

Abstract— The reflection properties of a display device influence the available contrast and affect the perception of low-luminance detail. We report on a Monte Carlo method for modeling the bidirectional reflectance of multi-layer structures used in thin-film organic light-emitting displays. The results show a predominant specular peak along with a quasi-Lambertian component and significant haze.

I. INTRODUCTION

The effective physical contrast of display devices is affected by the achievable contrast generated by the light-producing or light-modulating elements, and by reflections of ambient light. In emissive displays that are typically highly reflective by design, the control of ambient light reflection is critical to achieve high contrast, especially when large luminance dynamic range is needed. For instance, in high-performance medical imaging cathode-ray tubes (CRTs), the glass faceplate is darkened to reduce diffuse reflections and is coated with an anti-reflection film to reduce the specular component. Previously, we studied the effect of display reflectance on the physical contrast in the low luminance end of the grayscale, and related human visual system performance to the maximum ambient illumination that maintains a perceptually linear luminance scale [1]. It has been shown that, for CRTs, the display reflectance can be characterized by the sum of two components: specular and diffuse reflections. However, in flat-panel displays, the complete description of reflectance is more complex and requires the evaluation of the bidirectional reflection distribution function (BRDF) [5, 11].

In this paper, we describe a computational method for modeling the BRDF of electronic displays that relies on an optical Monte Carlo simulation code developed to study light transport processes in emissive structures. We compute the angular emission distribution for a beam incident into devices having different structures. We present re-

AB (agb@cdrh.fda.gov) and RJJ are with the Center for Devices and Radiological Health of the U.S. Food and Drug Administration, Rockville, MD. SL and JK are with the Department of Electrical Engineering and Computer Science at the University of Michigan, Ann Arbor, MI. EFK is with the Flat Panel Measurement Laboratory of the National Institute of Standards and Technology, Gaithersburg, MD.

sults for Lambertian and specular surfaces, for CRT monitors and for organic light-emitting displays (OLEDs).

II. METHODS

A. Monte Carlo simulations

The BRDF calculations are based on a Monte Carlo (MC) method developed for studying light transport effects in emissive structures [1]. The MC method makes use of the generation of photons with random directions according to a probability distribution function that describes the nature of the light source [3, 8]. In this analysis, the light source is a collimated beam or a collimated, distributed planar source, incident on the display surface with a direction determined by (θ_i, ϕ_i) with a given wavelength distribution $S(\lambda)$, and polarization state p. The photon histories are followed through a sequence of events that includes absorption, scattering and Fresnel refraction. The simulation models bulk absorption events, optically thin coatings and rough surfaces. The outcome of each individual event is dependent on the photon energy and polarization, and on the material optical properties. Bulk absorption is determined by sampling the probability of photon absorption after a path of length l using an exponential law $P_{abs}(l) = 1 - e^{-\mu_{abs}(\lambda)l}$, where $\mu_{abs}(\lambda)$ is the wavelength-dependent linear absorption coefficient. At the optical boundaries, an analysis is performed depending on the surface type and material properties using Fresnel's equations with polarization dependance [7]. When the film thickness is comparable to the photon wavelength, we use modified Fresnel coefficients to describe the interference effects of optically thin films. The reflection and transmission coefficients are interpreted as probabilities, and therefore the photon is either transmitted or reflected. The simulation outcome is calculated by statistical average of the fate of all histories according to the desired quantity to be evaluated for each experiment. The angular distribution of all photons reflected by the device is constructed in bins with varying resolution to obtain satisfactory statistics per bin.

B. BRDF model

The BRDF, a formalism often used in optics [9], is defined for any reflecting object as the ratio of differential reflected luminance dL_o to the differential illuminance dE_i incident on the surface. In this work, we consider the reflectance from the display to be shift-invariant, or independent of position across the screen, therefore neglecting all edge-related phenomena. The complete expression is then given by a six-dimensional function:

$$BRDF(\theta_i, \phi_i, \theta_o, \phi_o, \lambda, p) = \frac{dL_o(\theta_o, \phi_o, \lambda, p)}{dE_i(\theta_i, \phi_i, \lambda, p)} \quad (1)$$

where λ is the photon wavelength and p is the polarization of the incoming light beam. The BRDF has units of sr^{-1}. The angle of incidence of ambient light is defined by (θ_i, ϕ_i), while (θ_o, ϕ_o) are the angles that define the direction of reflected light.

The precise evaluation of this function is time consuming and costly. The BRDF can be measured with a goniometric setup with fixed light source and variable detector, with variable source and fixed detector, or with a conoscopic approach where the directional intensity is mapped into a two-dimensional distribution recorded by a position-sensitive planar detector. The first two methods suffer from severe dependence of source and detector positioning precision which has to be less than $1°$. The third method requires expensive instrumentation.

The models of display devices presented in this paper are based on uniform slabs representing multiple material layers. In flat panel display devices, the specific details of the pixel structure influence reflection and propagation of light within the different layers. In this model, we incorporate the effect of device features at the pixel level into a general description of the scattering properties at the surface between the pixel circuits and the substrate. With this assumption, the light scattering processes can be considered radially-symmetric,[1] and the BRDF can be described by a function B' given by

$$B'(\alpha_i, \alpha_o, \lambda, P) = \frac{dL_o(\alpha_o, \lambda, P)}{dE_i(\alpha_i, \lambda, P)} \quad (2)$$

In this study, we consider only the integrated response to an unpolarized light source with flat spectrum in the range from 400 to 800 nm. Therefore, integrating over all λ and p for a given light source described by $S(\lambda)$ and p yields a simplified function

$$B^{\alpha_i}(\alpha_o) = dL_o(\alpha_o)/dE_i(\alpha_i) \quad (3)$$

[1] This assumption is not true for emissive displays with polarizer films or for liquid crystal displays. An extension of this work to include such structures is in progress.
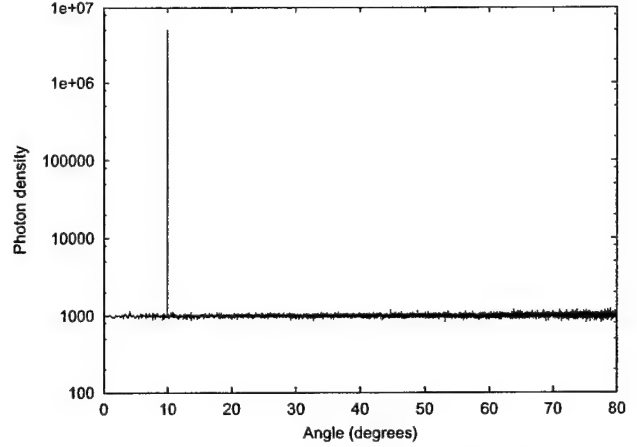

Fig. 1. $B(\alpha)$ for a surface with 50% specular and 50% diffuse components. The specular fraction results in a delta function at the specular angle of incidence (in this case $10°$). The correction with a factor equal to $cos(\alpha)$ yields a horizontal profile, typical of Lambertian surfaces.

Finally, the angular distribution function contained in equally spaced bins from the Monte Carlo simulations is reduced to a luminance distribution density in the range of $[0, 90°]$ for a given incidence angle α_i with a factor $1/cos(\alpha_o)$. The introduction of this factor is needed to directly relate the distribution density in angles with the expected angular variations in the luminance out of the device (L). $B^{\alpha_i}(\alpha_o)$ is also known as the in-plane or two-dimensional BRDF. Eq. 4 shows the final metric computed from the Monte Carlo simulations.

$$B^{\alpha_i}(\alpha_o) = \frac{dL(\alpha_o)/cos(\alpha_o)}{dE(\alpha_i)} \quad (4)$$

Let us consider a reflective surface for which half of the time photons are reflected specularly, and the rest of the time, undergo diffuse reflection according to a Lambertian distribution. For this case, the BRDF is known analytically and is given by Eq. 5, taking into account the number of histories (H) and the number of angular bins (β),

$$B^{\alpha_i}(\alpha_o) = \frac{1}{dE(\alpha_i)} \begin{cases} 0.5H & \alpha_o = \alpha_i, \\ \frac{1}{\beta}(2 \times 0.5 \times H) & \alpha_o \neq \alpha_i. \end{cases} \quad (5)$$

The factor of 2 comes from the summation of photons at positive and negative angles with respect to the surface normal. Fig. 1 shows the output angular distribution $B^{10}(\alpha_o)$ of an ideal Lambertian surface with a 50% specular component. The expected flat response of a Lambertian surface is seen in the simulation results. For this case, the number of angular bins provides an angular resolution of $0.009°$ ($\beta = 10^4$), therefore:
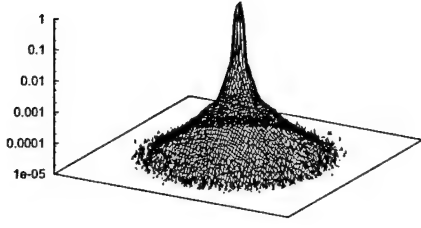
Fig. 2. Detected photon density using a 100×100 binning array corresponding to a high resolution monochrome CRT, simulated using a sensor array in close proximity to the display screen.

Fig. 3. $B^{10}(\alpha_o)$ for a monochrome CRT with geometrical and material models described in [1] for an incidence angle of $10°$ using $H = 10^6$.

$$B^{10}(\alpha_o) = \frac{1}{\beta} \begin{cases} 5 \times 10^6 & \alpha_o = 10°, \\ 10^3 & \alpha_o \neq \alpha_i. \end{cases} \qquad (6)$$

The dimensionless specular reflection coefficient R_S is approximately given by the ratio of the raw specular peak amplitude to the total number of histories:

$$R_S \approx \frac{number\ of\ photons\ in\ the\ specular\ peak}{total\ number\ of\ photon\ histories} \qquad (7)$$

which in this case is $R_S = 0.5$. Analogously, the diffuse reflection coefficient R_D (in nit/lux) can be approximated by the ratio of the fraction of non-specular photons over 2π to compensate for the emission into the hemisphere:

$$R_D \approx \frac{B^{10}(0)}{\beta} \frac{1}{2\pi} = 0.02\ sr^{-1} \qquad (8)$$

The corresponding detected photon density per pixel using a 100×100 binning array at the exit plane is shown in Fig. 2. The in-plane photon density is peaked at the center where the incident beam impinges on the display.

III. RESULTS

We present results for incident collimated sources at $10°$. We used a fixed light source with flat spectral distribution from 400 to 800 nm. For instance, Fig. 1 shows the output angular distribution of an ideal Lambertian diffuser surface with a 50% specular component. It can be shown that the specular reflection coefficient R_S is approximately given by the ratio of the raw specular peak amplitude to the total number of histories, and that R_D can be calculated using Eq. 8 [2].

To model typical high-performance medical imaging CRT monitors, we used a structure validated in previous work [3]. The CRT emissive structures consisted of an absorptive glass faceplate of 13 mm with a phosphor layer
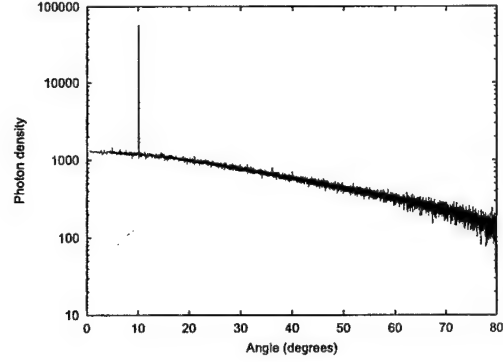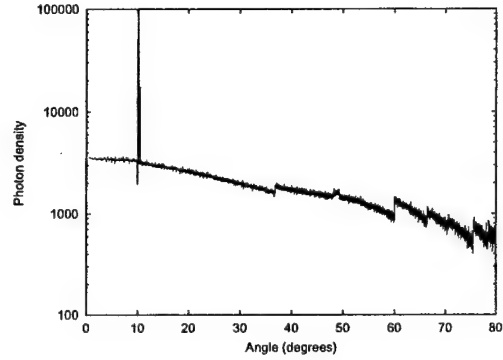

Fig. 4. $B^{10}(\alpha_o)$ for an OLED device with geometrical and material models described in [4] for an incidence angle of $10°$ using $H = 10^6$.

having a diffuse reflectance of 0.90-0.99, and an anti-reflective coating. Fig. 3 shows the specular and quasi-Lambertian components typical of CRTs. The value of the specular coefficient R_S calculated from the raw specular peak is around 0.045, and R_D is around 0.02 sr^{-1}. These values agree well with previous measurements of similar devices [1]. The decrease in luminance with angle can be associated with the absorption in the faceplate and most importantly, with the non-Lambertian nature of the reflections. We conclude from these results that the diffuse reflections (and possibly the emissions) from CRTs are more forward-peaked than would be the case for a perfect Lambertian diffuser. These results are consistent with recent observations reported by Blume [6] where the luminance of CRTs was measured at different viewing directions using a spot photometer.

Organic light-emitting displays are simulated using a typical structure model that includes measured optical properties for the organic polymer films and the substrate [4]. The OLED model represents a hetero-structure OLED described by He et al. [10] with an aluminum cathode electrode and a transparent anode ITO electrode (160
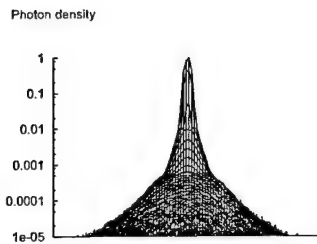
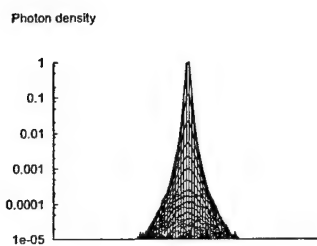Fig. 5. Normalized reflected spot profile for the CRT model.

Fig. 6. Normalized reflected spot profile for the OLED model.

nm, refractive index 1.8). The organic polymer film thickness used was 200 nm. The substrate index of refraction was 1.5 and its thickness 900 μm. Fig. 4 shows $B^{10}(\alpha_o)$ for OLEDs. It can be observed that the specular component is predominant ($R_S = 0.10$, $R_D = 0.06$ sr^{-1}). The results reveal that the specular peak has a significant width. This observation is consistent with an intermediate component of reflection observed in flat-panel displays or haze, caused by local light scattering. The spread of the specular peak shows the difficulty in defining specifically the specular and haze regions. We note that the diffuse component follows a quasi-Lambertian profile with about the same fall-off rate with off-axis angle found for the CRT models. We speculate that the several discontinuities are associated with refractive index changes of the different layers of the OLED stack. From the simulation results, it is possible to compute a haze ratio associated with the full width at half maximum of about 2°. However, as described in experimental studies, the value of the haze ratio is very sensitive to the cut-off limit. In Figs. 5 and 6, we show a comparison of the simulated reflected beam spot profiles for the CRT and OLED model. The significant diffuse reflections off the CRT phosphor layer cause blur. For the OLED model, the mirror-like appearance of the reflected spot is consistent with a small diffuse component.

IV. DISCUSSION

We present a novel method based on Monte Carlo techniques to calculate the bidirectional reflectance distribution function of emissive displays. We demonstrate the validity of the results using simple models for which the exact analytical solution is known, and by comparing the results with experimental measurements. We conclude that for both emissive display technologies, the reflections are slightly more forward-peaked than the predictions of Lambertian profiles. We show that the BRDF of OLED displays based on polymer films backed with a metallic reflective electrode is highly specular. We report for the first time the complete BRDF signature of OLEDs, showing that the haze component is small, with a characteristic width of 2°. This intermediate component of reflection complicates the measurement of the specular peak since luminance meters having slightly different apertures will produce a specular reflection component with large errors. This modelling tool will be used to demonstrate improvements of novel designs for achieving high-contrast in high-illuminance environments without the need to fabricate test devices, or use expensive instrumentation. We are investigating the effect of the optical properties and absorptive layers on the reflectance properties of OLEDs, and the BRDF signatures of liquid crystal displays.

REFERENCES

[1] A. Badano. *Image Quality Degradation by Light Scattering Processes in High Performance Display Devices for Medical Imaging*. PhD thesis, University of Michigan, 1999.

[2] A. Badano. Monte Carlo modeling of the bidirectional reflectance of display devices. *In preparation*, 2001.

[3] A. Badano, M. J. Flynn, E. Muka, K. Compton, and T. Monsees. The veiling glare point-spread function of medical imaging monitors. In *Proceedings of the SPIE Medical Imaging Display Conference*, 1999.

[4] A. Badano and J. Kanicki. Monte carlo analysis of the spectral photon emission and extraction efficiency of organic light-emitting devices. *Journal of Applied Physics*, 90(4), 2001.

[5] M. E. Becker. Evaluation and characterization of display reflectance. *Displays*, 19:35–54, 1998.

[6] H. Blume. In *Proceedings of the SPIE Medical Imaging Conference*, volume 4323-07, 2001.

[7] M. Born and E. Wolf. *Principles of Optics*. 3rd revised edition, 1965.

[8] J. Delacour, S. Ungar, G. Mathieu, G. Hasna, P. Martinez, and J.-C. Roche. Front panel engineering with CAD simulation tool. In *Proceedings of the SPIE Flat Panel Display Technology and Display Metrology Conference*, 1999.

[9] M. Elias, L. Simonot, and M. Menu. Bidirectional reflectance of a diffuse background covered by a partly absorbing layer. *Optics Communications*, 191:1–7, 2001.

[10] Y. He, S. Gong, R. Hattori, and J. Kanicki. *Applied Physics Letters*, 74, 1999.

[11] E. F. Kelley. Display reflectance model based on BRDF. *Displays*, 19:27–34, 1998.

MONTE CARLO SIMULATION OF SPECTRAL PHOTON EMISSION OF THE ORGANIC POLYMER LIGHT-EMITTING DEVICES

Shu-jen Lee, [a), b) *] Aldo Badano,[c)] Yongtaek Hong,[a)] and Jerzy Kanicki[a)]

[a)] *Organic & Molecular Electronics Laboratory, Department of Electrical Engineering and Computer Science, The University of Michigan – Ann Arbor, MI 48109*
[b)] *Macromolecular Science and Engineering Center, The University of Michigan – Ann Arbor*
[c)] *U. S. Food and Drug Administration, Center for Devices and Radiological Health, Rockville, MD.*

Abstract

We reported a Monte Carlo method for modeling the light transport phenomena in the organic polymer light-emitting devices (OP-LEDs) fabricated on plastic substrates. The OP-LED consists of a combination of a hole transport layer (HTL) of PEDOT/PSS and a light-emitting layer of Dow Chemical green B or red B organic polymer, Fig. 1. In this simulation we assumed a point light source having photon emission spectra represented by photoluminescence (PL) spectra of the organic polymers. This simulation method describes the fate of photons through multiple scattering events determined by the wavelength-dependent material optical properties in a 3-D Cartesian geometry, thus considering the effects of refraction at different interfaces, back-reflection, and absorption within the polymer layers. The absorption coefficients, $\mu(\lambda)$, used in this simulation work were measured by a combination of the UV-visible absorption and the photothermal deflection spectroscopy, and the refractive indices, $n(\lambda)$, were obtained by spectroscopic ellipsometry.

We apply this method to analyze the light wavelength distribution and extraction efficiency. We found that the simulated light emission spectra of the green and red light-emitting devices are very similar to the measured PL spectra, Fig. 2. We also established that the calculated extraction efficiency for the red (η_{ext}=21.71%) and green (η_{ext}=21.70%) OP-LEDs are approximately the same. We further investigated the light emission angular distribution of the OP-LEDs, and found that the angular distribution is rather a pseudo-Lambertian than Lambertian with increased intensity in the forward direction, Fig. 3. It was found that the light refraction at different interfaces leads to this pseudo-Lambertian angular distribution, while the absorption and the back-reflection have minor effects. Finally, it is clear from our simulation that the waveguiding effect cannot be neglected in the OP-LEDs and its contribution will be dependent on substrate thickness and refractive index values.
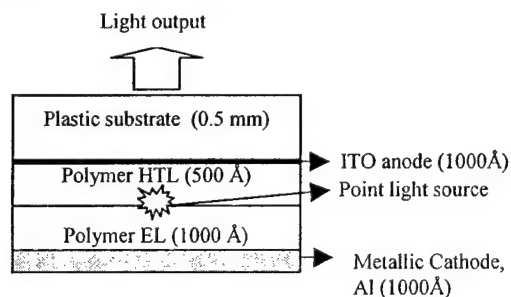
Fig. 1: The cross-section of the device structure used in this simulation work (not to scale).
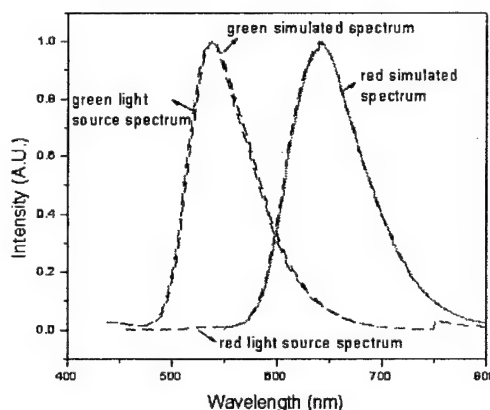

Fig. 2: The simulated light output spectra of the OP-LEDs. The PL spectra for green B and red B organic polymers are also shown in this figure.
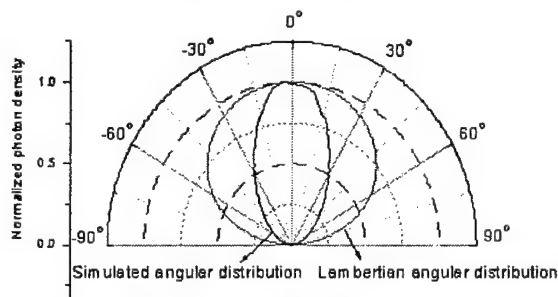

Fig. 3: The simulated light emission angular distribution of the OP-LEDs.

* Corresponding author: Shu-jen Lee, 1049 BIRB, 2360 Bonisteel Blvd., Ann Arbor, MI 48109-2108. Phone: (734)9360972, fax: (734)6152843, e-mail: shujen@umich.edu

Monte Carlo Simulation of Spectral Photon Emission of the Organic Polymer Light Emitting Devices

Shu-jen Lee[a), b)], Aldo Badano[c)], Yongtaek Hong[a)], Jerzy Kanicki[a)], and Hsu-ting Huang[a)]

a) Organic & Molecular Electronic Laboratory, Department of Electrical Engineering and Computer Science, University of Michigan, Ann Arbor, MI 48109
b) Macromolecular Science and Engineering Center, University of Michigan
c). U. S. Food and Drug Administration, Center for Devices and Radiological Health, Rockville, MD

MOTIVATION

Optimization of the OP-LED structure by optical design and modeling
- To understand the light transport process within the device
- To increase the device photon extraction efficiency
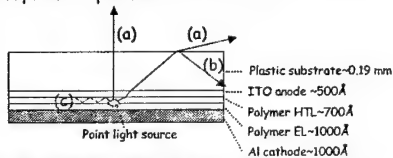- To enhance display contrast ratio

MONTE CARLO LIGHT TRANSPORT SIMULATION METHOD

Features:
- Tracks individual photons as particles from luminescent center to fate
- Output from statistically averaged quantities
- Flexible, accurate and fast
- Source: spatial (point, 2D or 3D distributed), directional (isotropic, Lambertian, pencil beams), energy (sampled from pdfs)
- Material properties: refractive index, $n(\lambda)$, and linear absorption coefficients, $abs(\lambda)$
- Polarization tracking
- Surface: absorptive, reflective, optically thin-film, rough surface

OP-LED structure used
- Light scattering phenomena (photon extraction (a), wave-guiding and edge emission (b), interference effect by thin films, and absorption (c)
- Assumptions: experimental material data

Plastic substrate~0.19 mm
ITO anode ~500Å
Polymer HTL~700Å
Polymer EL~1000Å
Al cathode~1000Å
Point light source

The photon extraction efficiency
- Fraction of photons that exit the device through the front plate, towards the viewers

$$\eta_{PE} = \frac{\text{number of photons that exit thru the front}}{\text{total number of histories}}$$
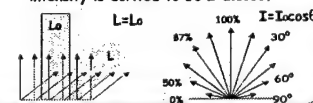
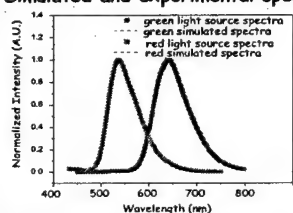$$\eta_{PE} + \eta_{waveguide} + \eta_{absorption} = 1$$

Input material data
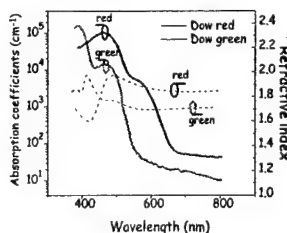
Definitions

Isotropic point source:
- Same luminous intensity (I, lm/sr) when viewing from any direction, $I = I_0$.

$$I = I_0$$

Lambertian surface:
- Same luminance (L, lm/m²/sr) when viewing from any direction, $L = L_0$. The luminous intensity is derived to be $I = I_0 \cos\theta$.
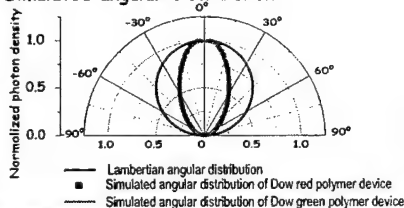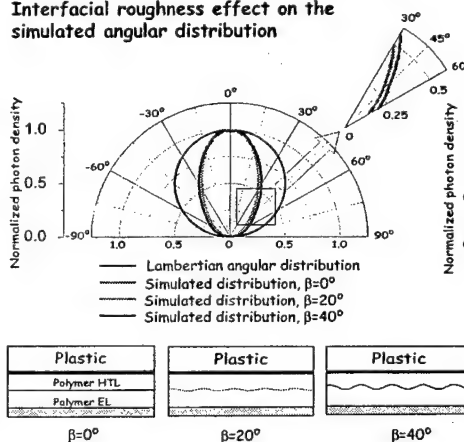
$$L = L_0 \qquad I = I_0 \cos\theta$$

RESULTS

Simulated and experimental spectra

Simulated angular distribution

— Lambertian angular distribution
■ Simulated angular distribution of Dow red polymer device
— Simulated angular distribution of Dow green polymer device

Interfacial roughness effect on the simulated angular distribution

— Lambertian angular distribution
— Simulated distribution, β=0°
— Simulated distribution, β=20°
— Simulated distribution, β=40°

Plastic	Plastic	Plastic
Polymer HTL		
Polymer EL		
β=0°	β=20°	β=40°

Experimental angular distribution

— Experimental angular distribution of a standard Lambertian light source
● Experimental angular distribuiton of a red polymer device
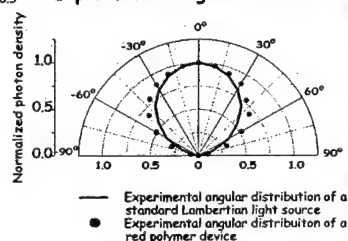
CONCLUSIONS

- A Monte Carlo method was uesd for modeling the light transport phenomena of the organic polymer light emitting devices
- The caculated extraction efficiencies for the red and green polymer devices are ~ 21.7%
- The simulated output angular distribution is a quasi Lambertian angular distribution with forward peaked intensity
- Further research is needed to qualify this simulation method for optimization of the OP-LED

Monte Carlo analysis of the spectral photon emission and extraction efficiency of organic light-emitting devices

Aldo Badano[a)] and Jerzy Kanicki[b)]

Solid-State Electronic Laboratory, Department of Electrical Engineering and Computer Science, The University of Michigan, Ann Arbor, Michigan 48109

We report on a Monte Carlo method for modeling light transport phenomena in multilayer organic polymer light-emitting devices on plastic flexible substrates. The method allows modeling of Cartesian geometrical structures describing the fate of photons through multiple scattering events determined by the wavelength-dependent material optical properties. We apply the method to analyze the wavelength distribution of emitted light spectra. We find that for all organic polymers considered, the light emission is slightly shifted toward the longer wavelengths, and that this shift is maximum for light emissions with peaks around 530 nm. The photon extraction efficiency is higher (0.430) for organic polymers emitting in the longer wavelengths, while the photon absorbed fraction is higher (0.676) for spectra with a maximum in the short wavelengths. © *2001 American Institute of Physics.* [DOI: 10.1063/1.1385571]

I. INTRODUCTION

The increase in the luminous efficiency of organic light-emitting devices (OLEDs) remains the focus of many efforts centered mostly on controlling charge transport and increasing the photoluminescent efficiency of organic materials. Currently, the analysis of the optical transport processes in OLEDs has obtained much attention. It is known that only about one fifth of the light generated in an OLED is emitted through the top surface of a simple OLED structure on a glass substrate.[1] The optical losses are related to absorption in the organic material and edge emission of waveguided modes. For a typical organic semiconductor with refractive index of 2.0, the escape cone angle into a substrate with an index of 1.5 is 48.6° which corresponds to a solid angle of only ~6%. Several attempts have been made to reduce the waveguided light fraction by using structured surfaces[2–4] and films,[5] and spherical scatterers within the organic film.[6] In addition to affecting the efficiency of the OLED, photon transport processes influence the spectral and angular distributions of the emitted light intensity. Both distributions are important design parameters for achieving full-color efficient OLEDs for flat-panel display applications.

After the simple analysis of OLED efficiency presented in Ref. 1, several groups have investigated the effect of light transport in multilayer structures.[3,7–9] The method we present in this article is based on a Monte Carlo (MC) approach.[10,11]

II. SIMULATION METHOD

The MC method makes use of the generation of photons with random direction according to a distribution function describing the nature of the light emission. In this analysis,

the light source within the organic polymer layer is considered isotropic from a single point situated in the center of the device (see Fig. 1). To obtain an isotropic distribution of the directional cosines, we sample the three directional cosines that define the photon direction according to

$$C_x = \sqrt{1 - \xi_1^2} \sin 2\pi\xi_2,$$

$$C_y = \sqrt{1 - \xi_1^2} \cos 2\pi\xi_2,$$

$$C_z = \xi_2,$$

where ξ_1 and ξ_2 are uniformly sampled in [0,1). The energy of the photon source is defined by a table that corresponds to a specific spectral light emission. The initial photon polarization vector is sampled uniformly in the 4π space, therefore assuming unpolarized light emission. The photon histories are then followed through a sequence of interactions that includes absorption and Fresnel refraction. A unique advantage of this simulation method is its ability to model bulk absorption events, thin-film coatings and rough surfaces, while keeping track of the photon polarization state. Bulk absorption is determined by sampling the probability of a photon being absorbed after a path of length l by the exponential law

$$P(l) = 1 - e^{-\mu_{ab}(\lambda)l},$$

where $\mu_{ab}(\lambda)$ is the wavelength-dependent linear absorption coefficient. At the optical boundaries, an analysis is performed depending on the surface type and material properties using Fresnel's equations and considering the polarization of the incoming photon.[12] When the film thickness is comparable to the photon wavelength, we use modified Fresnel coefficients to describe the interference effects of optically thin films. The reflection and transmission coefficients are then interpreted as probabilities. The simulation outcome is calculated by a statistical average of the fate of all histories according to the desired quantity to be evaluated

[a)]Current address: U.S. Food and Drug Administration, Center for Devices and Radiological Health, 12720 Twinbrook Parkway, Rockville, MD 20857; Electronic mail: agb@cdrh.fda.gov

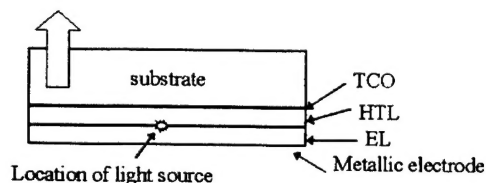[b)]Electronic mail: kanicki@eecs.umich.edu

FIG. 1. Schematic cross section of the OLED structure used for the Monte Carlo simulations, showing the location of the centered point light source at the interface between the hole-transporting and emissive organic polymer layers.

FIG. 2. Refractive index and normalized absorption coefficient of organic polymers A, B, and C modeled in this work.

for each experiment. Possible reporting options include the angular and spectral distributions of the emitted photons, the point-spread function, the specular and diffuse reflection coefficients, and a summary of scattering event statistics.

From the light emission at the luminescent center until the photons emerge, multiple scattering events take place within the multilayer OLED structure. For the purpose of our analysis, we define the device external quantum efficiency as

$$\eta_E = \eta_{in} \eta_{pe},$$

where η_{in} is the intrinsic quantum efficiency related to carrier recombination and photoluminescent fraction, and η_{pe} is the photon extraction efficiency. We introduce η_{pe} to represent the probability that a photon generated at the luminescent center within the OLED, emerges through the front surface of the device (through the transparent electrode), thereby contributing to luminance. The η_{pe} depends strongly on the device structure and on the material and surface properties, and is always less than unity due to light absorption, waveguiding, and edge emissions. We can summarize the relevant physical processes that occur as

$$\eta_{pe} = 1 - \eta_{wa} - \eta_{ab} - \eta_{tr},$$

where η_{wa} is the fraction of photons that are waveguided within the structure and exit through the device edges, η_{ab} is the absorbed fraction, and η_{tr} is the fraction transmitted through the metallic electrode deposited in the side opposite the direction of the desired light emission. The top metallic cathode electrode of all the OLED structures modeled in this article is an aluminum layer deposited by vacuum evaporation.[13] We considered $\eta_{tr} = 0$ in all simulations presented in this article. In this work, we neglected the photoluminescence quenching due to polymer composition or blend variations and the presence of carrier flow within the OLED. Electric field induced photoluminescence (PL) quenching in conjugated polymers, which is caused by exciton dissociation, is well known,[14] but cannot be implemented easily in this calculation. It should be noted that this PL quenching is not important at the OLED operating point.

III. RESULTS AND DISCUSSION

We measured the index of refraction, absorption, PL, and electro-luminescence (EL) of three organic polymers (A, B, and C) with peak emissions in a different region of the visible spectrum. The refractive index (considered equal for the three organic polymers) and absorption characteristics are shown in Fig. 2. We used the PL spectrum as the photon
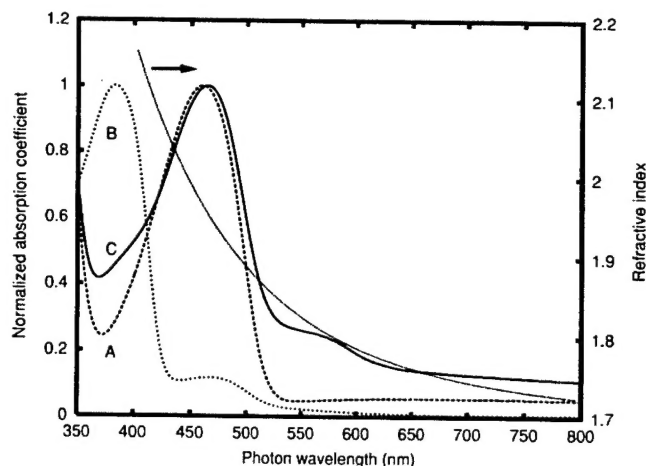
energy distribution at the source for the MC histories. The OLED structure modeled in this article (see Fig. 1) is a heterostructure OLED described by He et al.[13] as one with an aluminum cathode electrode and a transparent anode ITO electrode (160 nm, refractive index of 1.8). The organic polymer film thickness used was 200 nm. The transparent substrate index of refraction was 1.5 and its thickness was 900 μm.

In Fig. 3, we present results of the simulated light (SL) emission wavelength distribution. For the three PL spectra considered, the measured EL spectrum is only slightly shifted toward the longer wavelengths. Our MC simulation results are consistent with this trend. By computing separately the simulated emission from a device structure having absorption in the organic polymer film, and from another with no absorption but with a thin-film transparent layer between the organic material and the substrate, we have confirmed that the decrease in power efficiency of the shorter wavelength range is associated with absorption in the organic material, while the increase in strength at longer wavelengths is caused by interference effects associated with the transparent conductive coating. Our simulation method can correctly predict the shift in maximum wavelength of each EL spectrum with respect to the PL spectrum of each material. It should be noticed that the maximum of the SL spectrum of each material is located very close to the corresponding maximum of the measured EL spectrum. However, especially in the longer wavelengths, a discrepancy exists between the EL and the MC calculated SL that cannot be explained in terms of optical transport phenomena. The discrepancy between the SL and EL suggests that the spectral light emission at the source might not be completely accurate. For our MC simulations, we have assumed that the spectrum at the source is equal to the PL spectrum measured for each polymer. The actual light emission in OLEDs could differ from that of the PL, reflecting the geometrical and structural differences in both the solid-state films in the OLED and in the device structure. Photoluminescence quenching due to the presence of carriers might also affect the spectral emission by modifying the ratio between radiative and nonradiative recombination.
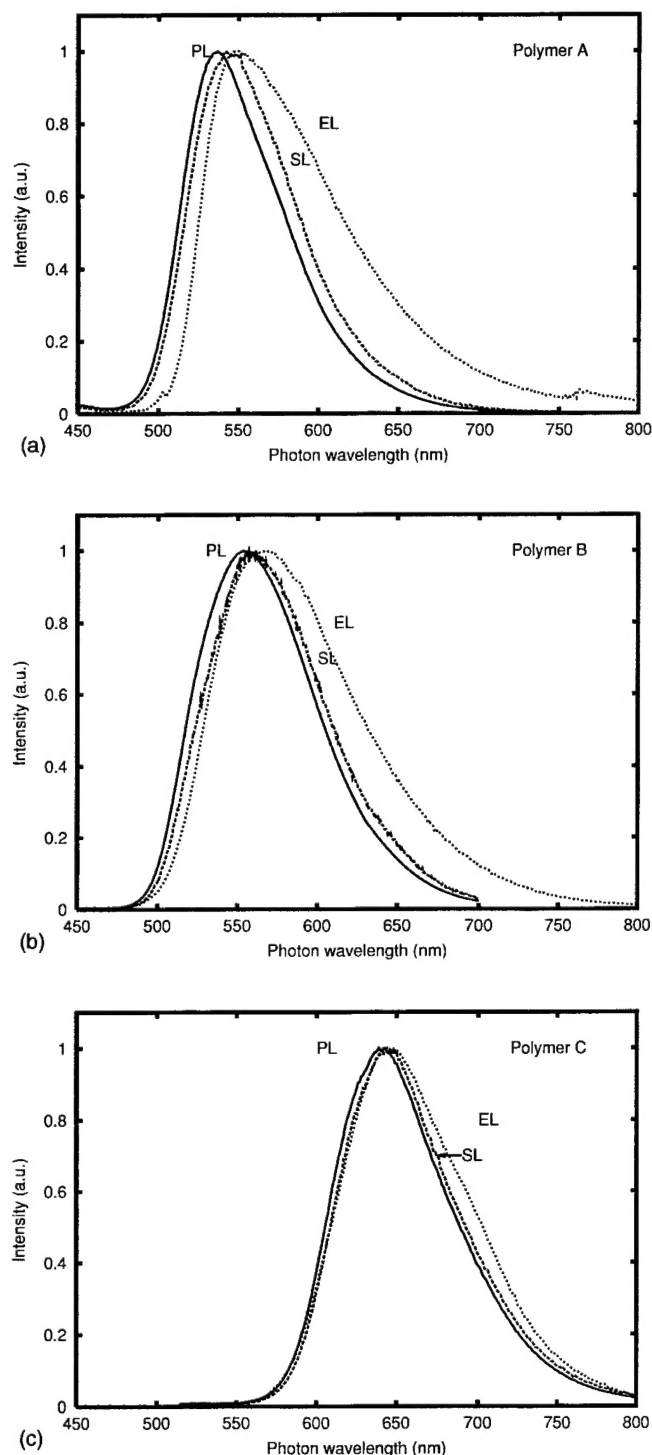
(a)

(b)

(c)

FIG. 3. Photoluminescent, electroluminescent, and simulated light emission spectra of organic polymers A, B, and C.

(a)

(b)

FIG. 4. Extraction efficiency η_{pe}, waveguiding η_{wa}, and absorption η_{ab} for different transparent conductive oxide electrode models: (a) effect of refractive index, and (b) effect of thin-film thickness. The vertical line represents the default values for the refractive index and thickness of the transparent electrode used for the calculations of the light emission spectra shown in Fig. 3. Curves are shown for each of the three polymers modeled in this article (A, B, and C).

In general, it is expected, and was experimentally confirmed for our OLEDs, that the intensity of the PL spectrum decreases with increasing applied voltage (e.g., with increasing current density). However, this decrease is not very large. Furthermore, it is expected that the light emission from excimers can contribute to the EL spectrum at longer wavelengths. This contribution will depend on the polymer structure and will be significant in copolymers. We have checked experimentally that the PL spectra shape is independent of
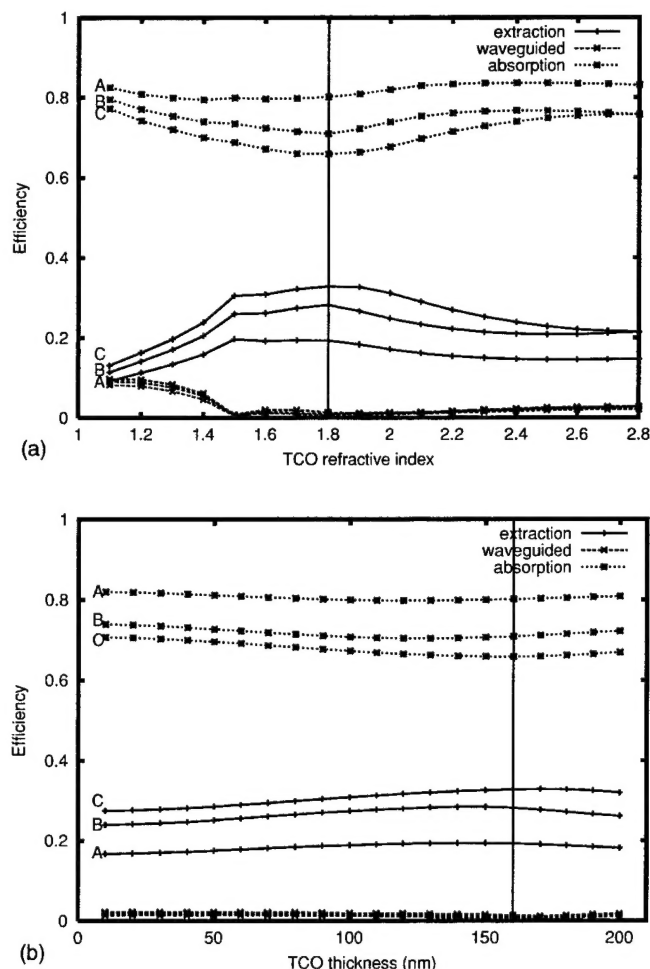
film thickness. We have also verified through simulation that the film thickness of the EL layer and the location of the light-emitting source within the OLED structure do not affect either the EL spectra shape or the peak maximum location.

The extraction efficiency η_{pe} is also affected by the wavelength distribution of the photon source. For the case of a transparent electrode having a thickness of 160 nm and a refractive index of 1.80, η_{pe} is 0.314 for polymer A, 0.334 for polymer B, and 0.430 for polymer C. The absorbed fraction η_{ab} is 0.676, 0.655, and 0.553, and the wave-guided fraction η_{wa} is 0.001, 0.011, and 0.017, respectively, for polymers A, B, and C. The low η_{wa} is caused by high absorption in the organic film. In Fig. 4, we present results showing the change in the values of η_{pe}, η_{ab}, and η_{wa} with the index of refraction (thickness) of the transparent conducting oxide (TCO) electrode covering the range from 1.1 to 2.7 (10–200 nm). We find that both the thickness and the refractive index of the transparent electrode have a minor effect on the shift of the SL spectrum with respect to the PL emission. We obtained a maximum η_{pe} for a TCO thickness and a refractive index of about 170 nm and 1.85, respectively.
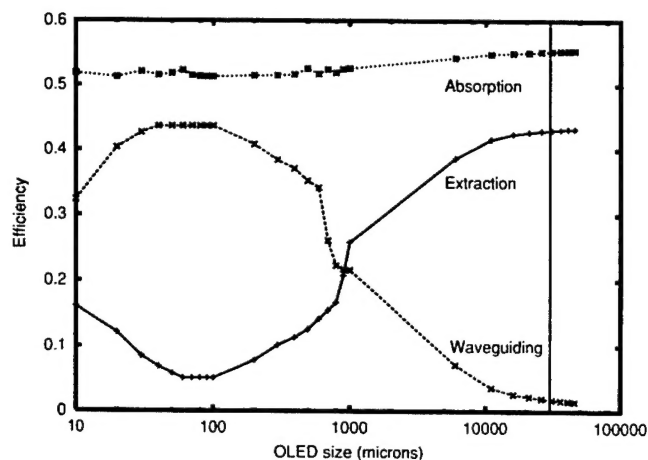
1830   J. Appl. Phys., Vol. 90, No. 4, 15 August 2001

A. Badano and J. Kanicki

FIG. 5. Extraction efficiency η_{pe}, waveguiding η_{wa}, and absorption η_{ab} as a function of OLED size for polymer B. Similar curves were obtained for polymers A and C. The vertical line represents the default device size used throughout this article.

The waveguide modes are determined by the geometry of the OLED stack that defines a total internal reflection (TIR) angle (α_{TIR}) with respect to the device plane, beyond which all photons are emitted through the edges. Since our source of photons is isotropic, we expect lower η_{wa} for larger devices due to (1) an increased probability of reflection and scattering going into the solid angle defined by α_{TIR}, and (2) increased absorption in the organic polymer layer. The simulation result presented in Fig. 5 confirms this assumption. For OLED sizes larger than 50 μm, η_{pe} steadily increases because more photons impinge directly (as a first interaction) into the substrate. For small device sizes below 2 mm, the absorbed fraction η_{ab} remains constant while the waveguiding decreases as the photon extraction efficiency increases. When the device size decreases below 100 μm, lateral boundary conditions become important and edge effects are observed. In our simulations, no additional structure is present at the edges of the device (i.e., the sides are considered to be smooth surfaces in contact with air). Photons reflected from the sides of the substrate at larger angles with respect to the surface normal have a larger probability of exiting the device through the top surface, thereby contributing to the extraction efficiency and to the luminance. For large device sizes, η_{pe} and η_{ab} increase while the waveguiding continues to decrease at a faster rate. The results also confirm that since most of the photon waveguiding occurs in the transparent substrate, the absorption in the organic polymer film has a minor effect on reducing the light edge emission and increasing the photon extraction efficiency.

IV. CONCLUSION

In this article, we have presented a method to model light transport processes in OLEDs based on Monte Carlo techniques. For all organic polymers considered in this work, our results show that the simulated light emission is shifted toward the longer wavelengths, consistent with experimental measurements of EL. We also showed that the photon extraction efficiency is reduced by light absorption and waveguiding. Reduction of the OLED waveguided fraction can be obtained by using structured substrates or by tuning the refractive index of the layers to maximize the transmission and reduce the total internal reflection at each interface. Of particular importance to this approach is the interface between the organic polymers and the TCO/substrate, as well as details of the structure and index of refraction of the layers in plastic substrates. The presence of optimized thin-film coatings in a plastic substrate could contribute to a decrease in internally reflected trapped photons. A combination of these two approaches could result in optimal OLED structures with high photon extraction efficiency.

ACKNOWLEDGMENTS

[1] N. C. Greenham, R. H. Friend, and D. D. C. Bradley, Adv. Mater. **6**, 491 (1994).

[2] I. Schnitzer, E. Yablonovitch, C. Caneau, T. J. Gmitter, and A. Sherer, Appl. Phys. Lett. **63**, 2174 (1993).

[3] G. Gu, D. Z. Garbuzov, P. E. Burrows, S. Venkatesh, and S. R. Forrest, Opt. Lett. **22**, 396 (1997).

[4] R. Windisch, P. Heremans, A. Knobloch, P. Kiesel, G. H. Döhler, B. Dutta, and G. Borghs, Appl. Phys. Lett. **74**, 2256 (1999).

[5] J. M. Lupton, B. J. Matterson, I. D. W. Samuel, M. J. Jory, and W. L. Barnes, Appl. Phys. Lett. **77**, 3340 (2000).

[6] T. Yamasaki, K. Sumioka, and T. Tsutsui, Appl. Phys. Lett. **76**, 1243 (2000).

[7] F. Cacialli, S. E. Burns, and H. Becker, Opt. Mater. **9**, 168 (1998).

[8] S. E. Burns, N. C. Greenham, and R. H. Friend, Synth. Met. **76**, 205 (1996).

[9] V. Bulović, V. B. Khalfin, G. Gu, P. E. Burrows, D. Z. Garbuzov, and S. R. Forrest, Phys. Rev. B **58**, 3730 (1998).

[10] A. Badano, Ph.D. thesis, University of Michigan, Ann Arbor, MI, 1999.

[11] G. F. Knoll and T. F. Knoll, IEEE Trans. Nucl. Sci. **35**, 872 (1988).

[12] M. Born and E. Wolf, *Principles of Optics*, 3rd ed. (Pergamon, New York, 1965).

[13] Y. He, S. Gong, R. Hattori, and J. Kanicki, Appl. Phys. Lett. **74**, 2265 (1999).

[14] M. Deussen, M. Sheidler, and H. Bassler, Synth. Met. **73**, 123 (1995).